

# Quality Assurance on a custom SiPMs array for the Mu2e experiment

N. Atanov, V. Baranov, J. Budagov, Yu. I. Davydov, V. Glagolev, V. Tereshchenko, Z. Usubov  
Joint Institute for Nuclear Research, Dubna, Russia

F. Cervelli, S. Di Falco, S. Donati, L. Morescalchi, E. Pedreschi, G. Pezzullo\*, F. Raffaelli, F. Spinella  
INFN sezione di Pisa, Pisa, Italy  
(\* email: pezzullo@PI.INFN.IT)

F. Colao, M. Cordelli, G. Corradi, E. Diociaiuti, R. Donghia, S. Giovannella, F. Happacher, M. Martini,  
S. Miscetti, M. Ricci, A. Saputi, I. Sarra  
Laboratori Nazionali di Frascati dell' INFN, Frascati, Italy

B. Echenard, D. G. Hitlin, T. Miyashita, F. Porter, R. Y. Zhu  
California Institute of Technology, Pasadena, USA

F. Grancagnolo, G. Tassielli INFN sezione di Lecce, Lecce, Italy  
P. Murat

Fermi National Accelerator Laboratory, Batavia, Illinois, USA

**Abstract**—The Mu2e experiment at Fermilab will search for the coherent  $\mu \rightarrow e$  conversion on aluminum atoms. The detector system consists of a straw tube tracker and a crystal calorimeter.

A pre-production of 150 Silicon Photomultiplier arrays for the Mu2e calorimeter has been procured. A detailed quality assurance has been carried out on each SiPM for the determination of its own operation voltage, gain, dark current and PDE. The measurement of the mean-time-to-failure for a small random sample of the pro-production group has been also completed as well as the determination of the dark current increase as a function of the ionizing and non-ionizing dose.

**Index Terms**—High energy physics instrumentation, Radiation effects, Silicon radiation detectors, Nuclear physics

## I. INTRODUCTION

THE Mu2e experiment at Fermilab will search for the charged lepton flavor violating process of neutrino-less  $\mu \rightarrow e$  coherent conversion in the field of an aluminum nucleus [1]. Mu2e will reach a single event sensitivity of about  $2.5 \cdot 10^{-17}$  that corresponds to four orders of magnitude improvements with respect to the current best limit. The detector system consists of a straw tube tracker and a crystal calorimeter. The calorimeter was designed to be operable in a harsh environment where about 10 krad/year will be delivered in the hottest region and work in presence of 1 T magnetic field. The calorimeter role is to perform  $\mu/e$  separation to suppress cosmic muons mimicking the signal, while providing a high level trigger and a seeding the track search in the tracker. In this paper we present the calorimeter design and the latest R&D results.

## II. MU2E CUSTOM SiPM ARRAY

The Mu2e calorimeter is composed by two disks of 1348 un-doped parallelepiped CsI crystals of  $34 \times 34 \times 200$  mm<sup>3</sup> dimension, each one readout by two large area SiPM arrays [2].

We translated the calorimeter requirements [3] in a series of technical specifications for the SiPMs that are summarized in the following list:

- 1) a high gain, above  $10^6$ , for each monolithic ( $6 \times 6$ ) mm<sup>2</sup> SiPM cell;
- 2) a good photon detection efficiency (PDE) of above 20% at 310 nm to well match the light emitted by the un-doped CsI crystals;
- 3) a large active area that, in combination with the PDE, could provide a light yield of above 20 p.e./MeV;
- 4) a fast rise time and a narrow signal width to improve time resolution and pileup rejection;
- 5) a Mean to Time Failure (MTTF) of  $O(10^6)$  hours;
- 6) and a good resilience to neutrons for a total fluency up to  $10^{12}$  n-1MeV<sub>eq</sub>/cm<sup>2</sup>.



Fig. 1. Mu2e SiPMs from: Hamamatsu, SensL and AdvanSid.

A modular and custom SiPM layout (Mu2e SiPM in the following) has been chosen to satisfy these requirements. To well match the wavelength of the emitted light produced by the CsI crystals, which peaks at about 300 nm, the SiPM detection efficiency have been extended in the UV region. The configuration readout of 2 series of three  $6 \times 6$  mm<sup>2</sup> monolithic SiPMs  $50 \mu\text{m}$  pitch has been selected to overcome the issues related to the parallel connection that, due to the

large capacitance, could have spoiled the pileup rejection and the energy and time measurements.

The performance of the Mu2e SiPM from three international firms, see Figure 1: Hamamatsu [4], SensL [5] and AdvanSid [6] were studied to select the vendor for the final production.

### A. Quality assurance procedure

A semi-automatized test station was assembled in order to measure: gain, operational voltage,  $I_{\text{dark}}$  and PDE of each cell of the Mu2e SiPMs in order to provide also information about the homogeneity of the SiPM response. The station consisted of:

- source meter Keithley 6487 [7];
- pulse generator Agilent [8];
- microcontroller Arduino MEGA [9];
- scope LeCroy WaveRunner [10];
- LED @ 315 nm from Thorlabs [11];
- custom relay board;
- custom amplifier using 2 MAR8 [12] chips;
- SiPM  $3 \times 3 \text{ mm}^2$   $50 \mu\text{m}$  pixel pitch [13].

A LabView [14] executable to control the source meter and the boards (via the microcontroller). Figure 2 shows a scheme of the setup. A water chiller system was used to keep the SiPM temperature stable at  $20^\circ\text{C}$ .

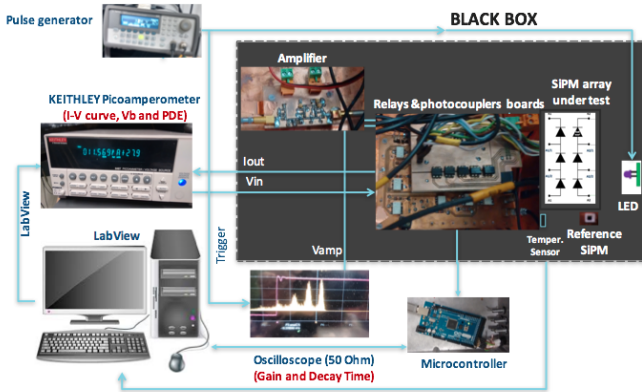


Fig. 2. Scheme of the semi-automatized station used for characterizing the Mu2e SiPMs.

For each cell of the Mu2e SiPMs we measured  $I_{\text{dark}}$  as a function of the bias voltage applied. This measurement allows to evaluate the breakdown voltage  $V_{\text{br}}$ , which corresponds to the peak position of the  $d \log I_{\text{dark}}/dV$ , and consequently the value of the  $I_{\text{dark}}$  at the operation voltage  $V_{\text{op}}$  that we set at  $V_{\text{br}}$ . Figure 3 shows an example of  $I$ - $V_{\text{bis}}$  scan with its logarithmic derivative.

Figure 4 shows on the left the distribution of the  $V_{\text{op}}$  of the Hamamatsu Mu2e SiPM-cells, while the plot on the right shows the distribution of the relative  $V_{\text{op}}$  Root-Mean-Square within each Mu2e SiPM. Figure 5 shows on the left the distribution of the  $I_{\text{dark}}$  of the same SiPM-cells and on the right the distribution of the  $I_{\text{dark}}$  Root-Mean-Square within each Mu2e SiPM under test. These measurements shows that

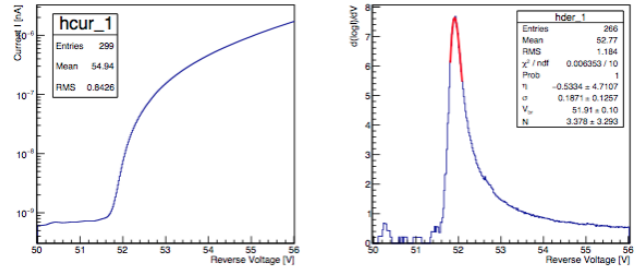


Fig. 3. Left:  $I$ - $V_{\text{bis}}$  scan. Right: distribution of  $d \log I_{\text{dark}}/dV$  with included a Fit to the curve for evaluating the  $V_{\text{br}}$ .

the Hamamatsu Mu2e SiPMs match the requirements on  $I_{\text{dark}}$  and  $V_{\text{op}}$  we specified on Section II.

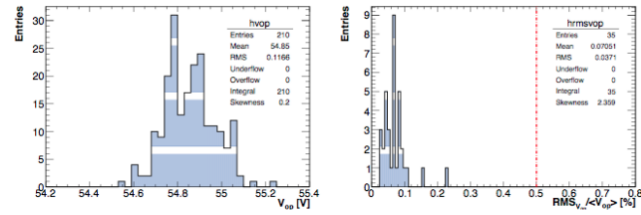


Fig. 4. Left: distribution of the  $V_{\text{op}}$  of all the Hamamatsu SiPM-cells. Right: of the relative  $V_{\text{op}}$  Root-Mean-Square within each Mu2e SiPM. The red line on the same plot show the 0.5% threshold we required.

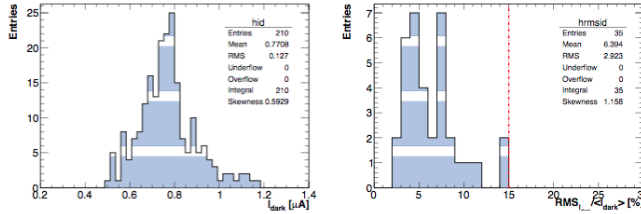


Fig. 5. Left: distribution of the  $I_{\text{dark}}$  of all the Hamamatsu SiPM-cells. Right: of the relative  $I_{\text{dark}}$  Root-Mean-Square within each Mu2e SiPM. The red line on the same plot show the 15% threshold we required.

The gain was measured at  $V_{\text{op}}$  using the technique described on reference [15]; the LED was set, using the waveform generator, in a condition where it was emitting a small amount of light (the mean number of emitted photons detected by the SiPM cell was  $\sim 1$ ), then the amplified SiPM signal was integrated in a fixed gate of 150 ns near the peak. The resulting charge distribution was finally use to evaluate the SiPM cell. Figure 6 shows on the left the distribution of the measured gain of all the SiPM-cells of the Hamamatsu Mu2e SiPMs, while on the right the gain Root-Mean-Square within each Mu2e SiPM. The red line on the left plot show the gain= $10^6$  threshold we required.

The PDE was measured by lighting the Mu2e SiPM under test and the SiPM used as reference with the 315 nm LED and then comparing the induced current in the two sensors. Figure 7 shows on the left the distribution of the measured PDE on all the Mu2e SiPM cells from Hamamatsu, while on the right the PDE Root-Mean-Square within each Mu2e SiPM.

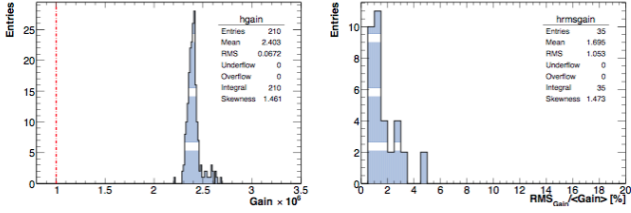


Fig. 6. Left: distribution of the gain of all the Hamamatsu SiPM-cells. The red line on the same plot shows the  $10^6$  threshold we required. Right: of the relative gain Root-Mean-Square within each Mu2e SiPM.

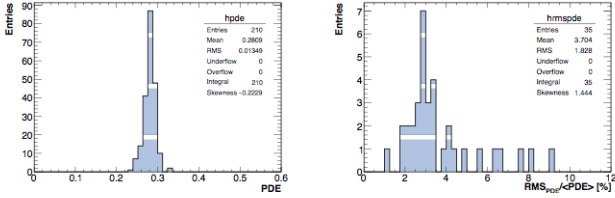


Fig. 7. Left: distribution of the PDE of all the Hamamatsu SiPM-cells. Right: of the relative PDE Root-Mean-Square within each Mu2e SiPM.

### III. RADIATION HARDNESS

One sample from each vendor was exposed to neutron fluence up to  $10^{12}$  n-1MeV<sub>eq</sub>/cm<sup>2</sup> at the Helmholtz-Zentrum Dresden-Rossendorf facility [16]. Figure 8 shows the experimental setup used to test the SiPM. During the whole irradiation period the SiPM were kept at 20°C and biased at their corresponding  $V_{op}$ . Figure 9 shows the trend of  $I_{dark}$

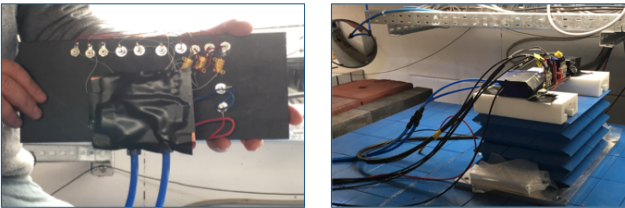


Fig. 8. Experimental setup used for the irradiation test.

as a function of the integrated neutron flux. Same plot shows that the Hamamatsu SiPM (red line) is more rad-hard w.r.t. the other two vendors.

### IV. MEAN TIME TO FAILURE

Five samples from each vendor were kept in a custom made thermostatic box operating at 50°C at their corresponding  $V_{op}$  (evaluated at the same temperature) for about 2556 hours to check that the SiPMs provide a MTTF of  $O(10^6)$ . We daily measured the  $I_{dark}$  and the charge response, pulsing UV light with a LED on the SiPMs, for all the samples during the entire period of test. Figure 10 shows the measured charge along the data taking period for the samples from Hamamatsu. Same plot shows that all the SiPMs were operative up to the end of the test.

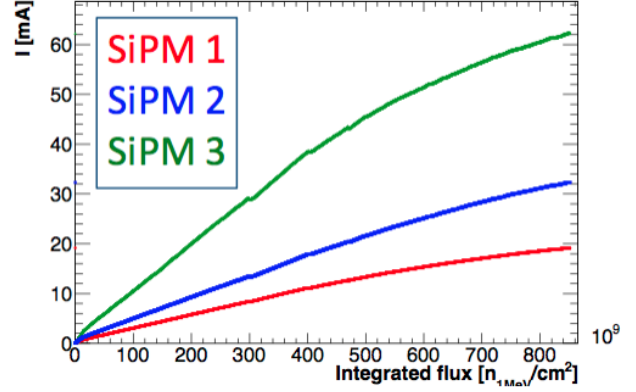


Fig. 9.  $I_{dark}$  versus the integrated neutron flux for the three vendors: red line is the Hamamatsu sample, blue line refers to the SensL one and the green line to the SiPM from AdvanSid.

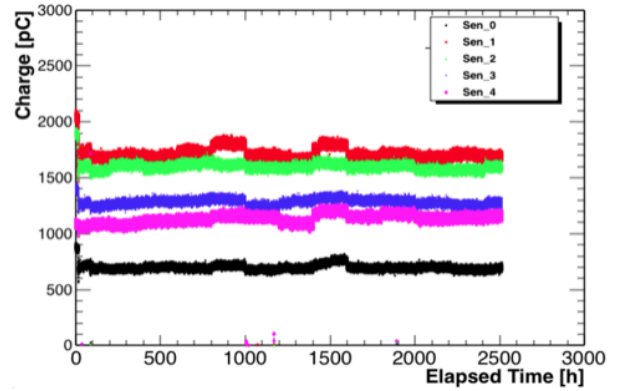


Fig. 10. Reconstructed charge, given in pC, of the 5 SiPMs from Hamamatsu under test versus the elapsed time during the MTTF test.

### V. SUMMARY

We showed the preliminary results of the SiPMs pre-production for the Mu2e calorimeter; 150 SiPM arrays were fully characterized with a semi-automatized station and operability of the devices was also tested under neutron fluence up to  $10^{12}$  n-1MeV<sub>eq</sub>/cm<sup>2</sup>. We also verified that the MTTF of these SiPM is larger than  $O(10^6)$ , thus satisfying the Mu2e technical requirements.

### ACKNOWLEDGMENT

This work was supported by the US Department of Energy; the Italian Istituto Nazionale di Fisica Nucleare; the US National Science Foundation; the Ministry of Education and Science of the Russian Federation; the Thousand Talents Plan of China; the Helmholtz Association of Germany; and the EU Horizon 2020 Research and Innovation Program under the Marie Skłodowska-Curie Grant Agreement No.690385.

## REFERENCES

- [1] L. Bartoszek *et al.*, *Mu2e Technical Design Report*, 3rd ed. arXiv:1501.05241 [physics.ins-det], 2014.
- [2] N. Atanov *et al.*, *Design and status of the Mu2e electromagnetic calorimeter*, NIM A, 824, 695-698, 2016.
- [3] Mu2e Calorimeter group, The Mu2e Calorimeter Final Technical Design Report, <http://mu2e-docdb.fnal.gov/cgi-bin/ShowDocument?docid=8429>
- [4] Hamamatsu, <http://www.hamamatsu.com/us/en/index.html>. Accessed: 2017.
- [5] SensL, <http://www.sensl.com>. Accessed: 2017.
- [6] AdvanSid, <http://advansid.com/home>. Accessed: 2017.
- [7] Keithley, source meter 6487 [http://download.tek.com/manual/6487-901-01\(B-Mar2011\)\(Ref\).pdf](http://download.tek.com/manual/6487-901-01(B-Mar2011)(Ref).pdf). Accessed: 2017
- [8] AGILENT, *33220A waveform generator*, [http://eclabslabs.njit.edu/student\\_resources/33220\\_user\\_guide.pdf](http://eclabslabs.njit.edu/student_resources/33220_user_guide.pdf). Accessed: 2017.
- [9] ARDUINO, *Arduino MEGA*, [http://www.atmel.com/Images/Atmel-2549-8-bit-AVR-Microcontroller-ATmega640-1280-1281-2560-2561\\_datasheet.pdf](http://www.atmel.com/Images/Atmel-2549-8-bit-AVR-Microcontroller-ATmega640-1280-1281-2560-2561_datasheet.pdf). Accessed: 2017.
- [10] LECROY, *WaveRunner 620Zi*, <http://cdn.teledynelecroy.com/files/pdf/waverunner-6zi-datasheet.pdf>. Accessed: 2017.
- [11] THORLABS, *UV LED with window*, <https://www.thorlabs.com/drawings/9dc48043db56b91c-4A2B20FA-A4DE-9249-0EB068B30EB26C54/LED315W-SpecSheet.pdf>. Accessed: 2017.
- [12] MINICIRCUITS, *MAR-8 monolithic amplifier*, <https://ww2.minicircuits.com/pdfs/MAR-8A.pdf>. Accessed: 2017.
- [13] HAMAMATSU, *SiPM S13360-6050CS*, [https://www.hamamatsu.com/resources/pdf/ssd/s13360\\_series\\_kapd1052e.pdf](https://www.hamamatsu.com/resources/pdf/ssd/s13360_series_kapd1052e.pdf)
- [14] E. Chance *et al.*, *National Instruments LabVIEW: A Programming Environment for Laboratory Automation and Measurement*, JALA, 12, 1, 17-24, 2007.
- [15] HAMAMATSU, *Hamamatsu technical note*, [http://www.hamamatsu.com/eu/en/community/optical\\_sensors/articles/measuring\\_characteristics\\_of\\_mppc/index.html](http://www.hamamatsu.com/eu/en/community/optical_sensors/articles/measuring_characteristics_of_mppc/index.html)
- [16] HZDR, *Helmholtz-Zentrum Dresden-Rossendorf*, <https://www.hzdr.de/db/Cms?pNid=0>. Accessed: 2017.